Thermal Strain Induced Temperature Compensation of Diode Lasers

Final Technical Report
12/15/97 – 12/15/00

P.I. - L.A. Coldren

ECE Technical Report #01-03

Air Force Office of Scientific Research
Contract No. F49620-98-1-0165

Department of Electrical and Computer Engineering
University of California at Santa Barbara, CA 93106-9560

REPORT DOCUMENTATION PAGE

Form Approved
OMB No. 0704-0188

1. AGENCY USE ONLY *(Leave blank)*	2. REPORT DATE	3. REPORT TYPE AND DATES COVERED
		FINAL DEC 15 97 TO DEC 15 2000

4. TITLE AND SUBTITLE
THERMAL STRAIN-INDUCED TERPERATURE COMPENSATION

5. FUNDING NUMBERS
61101E
D107/29

6. AUTHOR(S)
PROFESSOR COLDREN

7. PERFORMING ORGANIZATION NAME(S) AND ADDRESS(ES)
UNIVERSITY OF CALIFORNIA SANTA BARBARA

8. PERFORMING ORGANIZATION REPORT NUMBER
F49620-98-1-0165

9. SPONSORING/MONITORING AGENCY NAME(S) AND ADDRESS(ES)
AIR FORCE OF SCIENTIFIC RESEARCH
801 NORTH RANDOLPH ST RM732
ARLINGTON, VA 22203-1977

10. SPONSORING/MONITORING AGENCY REPORT NUMBER

11. SUPPLEMENTARY NOTES

12a. DISTRIBUTION AVAILABILITY STATEMENT

12b. DISTRIBUTION CODE

13. ABSTRACT *(Maximum 200 words)*

We have explored both monolithic and hybrid assembly techniques, with miniaturization the main goal in either case. The hybrid approach that we will describe makes use of a submount of dimensions comparable to those used on standard laser manufacturing, but made from a material chosen for a specific thermal expansion coefficient, either high or low compared to Inp, to obtain either enhanced or reduced temperature tuning. To increase the effectiveness of the differential expansion, we also developed a strain magnifying structure based on a deep crystallographic etch from the back of the substrate. One appeal of this hybrid technique is that the same basic technology can be applied to either tuning enhancement or reduction, by simply using a different submount. However, the ultimate in cost reduction and reliability would be obtained with a truly monolithic approach, and toward this end, we studied the properties of a high-expansion electroplated manganese film to serve as a stress inducing layer.

14. SUBJECT TERMS			15. NUMBER OF PAGES
			16. PRICE CODE
17. SECURITY CLASSIFICATION OF REPORT	**18. SECURITY CLASSIFICATION OF THIS PAGE**	**19. SECURITY CLASSIFICATION OF ABSTRACT**	**20. LIMITATION OF ABSTRACT**
UNCLASSIFIED	UNCLASSIFIED	UNCLASSIFIED	UL

Thermal Strain Induced Temperature Compensation of Diode Lasers

AFOSR Grant No. F49620-98-1-0165

Professor Larry A. Coldren, P. I.

Final Technical Report

December 15, 1997 to December 15, 2000

Department of Electrical and Computer Engineering

University of California

Santa Barbara, CA 93106

Introduction

Our goal in this program was to develop a practical technology to use temperature-dependent strain from differential thermal expansion to control the temperature-tuning rate of diode lasers for communications applications. We had previously demonstrated the feasibility of using such temperature-dependent strain to eliminate wavelength drift [1], and sought a manufacturable and reliable implementation. The original goal was to eliminate the need for thermoelectric coolers to stabilize the wavelength of lasers used for wavelength division multiplexed systems. Early in the program, Tom Koch at Lucent Technologies suggested that there was a strong interest in increasing the rate at which a DFB laser could be temperature-tuned, rather than decreasing it, so that a single TE–cooled laser could be used to transmit over several different WDM channels. We recognized that we could achieve this by simply changing the sign of the differential expansion.

We have explored both monolithic and hybrid assembly techniques, with miniaturization the main goal in either case. The hybrid approach that we will describe makes use of a submount of dimensions comparable to those used on standard laser manufacturing, but made from a material chosen for a specific thermal expansion coefficient, either high or low compared to InP, to obtain either enhanced or reduced temperature tuning. To increase the effectiveness of the differential expansion, we also developed a strain magnifying structure based on a deep crystallographic etch from the back of the substrate. One appeal of this hybrid technique is that the same basic technology can be applied to either tuning enhancement or reduction, by simply using a different submount. However, the ultimate in cost reduction and reliability would be obtained with a truly monolithic approach, and toward this end, we studied the properties of a high-expansion electroplated manganese film to serve as a stress inducing layer.

We demonstrated a 50% increase in the tuning rate $d\lambda/dT$ using a strain–magnified laser bonded to a high expansion submount [2]. This result verifies the concept, but is smaller than theoretically predicted, and too small to be of practical interest. The likely cause for the poor performance is unintentional bending of the laser under stress, and we discuss this issue in detail later.

We also demonstrated a 20% decrease in the tuning rate, using a similar laser bonded to a low expansion submount. This performance was also poorer than predicted, and probably for the same reasons. To eliminate the bending issue, we used a different technique to bond to the

submount, and incorporated an additional stress-inducing element. The result was a tuning rate near zero, albeit over a limited temperature range. Brittle fracture of the laser prevented operation over a wider temperature range.

It is this brittle fracture that appears to be the biggest problem now, and this is no surprise. While the calculated strains are within the idealized limits for elastic behavior, in practice the limits are much lower due to imperfections in the laser fabrication and bonding. We conclude that while the approach remains interesting, there are still difficult challenges to be met before a practical technology can be fielded.

Uniaxial Strain and Modal Wavelength

We have previously considered the effect of strain on the modal wavelength of a diode laser, and found that uniaxial strain along [1$\underline{1}$0] in 1.55 μm InGaAsP-InP lasers would lead to a change in the effective index of [1]

$$\frac{d\bar{n}}{d\varepsilon} = 2.29,$$

that is, a compressive strain of 1% reduces the effective index by .023. Since the modal wavelength is given by

$$\frac{d\lambda}{\lambda} = \frac{d\bar{n}}{\bar{n}},$$

the wavelength shift due to strain is

$$\frac{d\lambda}{d\varepsilon} = \frac{\lambda}{\bar{n}}\frac{d\bar{n}}{d\varepsilon}.$$

If we now consider the effects of temperature and temperature-dependent strain, we find

$$\frac{d\lambda}{dT} = \left.\frac{\partial\lambda}{\partial T}\right|_{\varepsilon} + \left.\frac{\partial\lambda}{\partial\varepsilon}\right|_{T} = \left.\frac{\partial\lambda}{\partial T}\right|_{\varepsilon} + \frac{\lambda}{\bar{n}}\frac{d\bar{n}}{d\varepsilon}\frac{d\varepsilon}{dT}.$$

For tuning reduction, we want $d\lambda/dT=0$, so the necessary strain rate becomes

$$\frac{d\varepsilon}{dT} = -\frac{1\bullet 10^{-4}}{K}.$$

For tuning enhancement, a doubling of the tuning may be obtained by simply changing the sign of the strain.

We are interested in generating the temperature dependent strain solely from differential thermal expansion, to avoid the need for separate temperature sensing, actuators, or feedback loops. However, the maximum thermal expansion of stiff materials is limited to about $2 \cdot 10^{-5}$/K, so that some form of strain magnification is needed. While simply lengthening the device would increase the total extension or contraction, the displacement would be distributed uniformly over the length, so the strain (fractional extension or contraction) would not change. If, however, the cross section of the device is made nonuniform, the stress and resulting strain may be concentrated at the region of narrower cross section. Then, the extra displacement arising from a longer device can effectively magnify the rate at which strain increases with temperature. We have analyzed this effect using the one-dimensional model shown in Fig. 1, in which a trench is etched into the substrate directly beneath the laser active region, and the substrate is bonded rigidly to a submount with a different expansion coefficient. We define a magnification factor, M, as

$$M = \frac{1}{\Delta\alpha}\frac{d\varepsilon}{dT},$$

where $\Delta\alpha$ is the difference in expansion between the laser substrate and the submount. We find

$$M = \left[\frac{L_1}{L_3} + \left(1 - \frac{L_1}{L_3}\right)\frac{X_1}{X_2} + \frac{E_1 X_1}{E_3 X_3}\right]^{-1},$$

where E_1, E_3 are Young's modulii of the laser and submount respectively, and the lengths L_i are as shown in the figure. The first term is the magnification expected if the unetched portion of the substrate and the submount are perfectly rigid, so that all of the strain is in the etched portion of the laser. The second term is a reduction due to the finite compliance of the unetched substrate, and the third term is a further reduction due to the compliance of the submount. The net magnification is shown in Fig. 2, assuming a submount thickness much greater than the laser substrate thickness so that the third term may be neglected. We see that the effect of the first term saturates quickly, unless the cross sectional ratio X_2/X_1 is large.

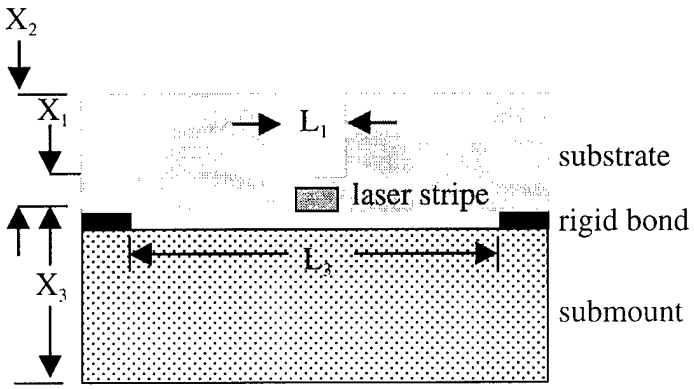

Fig. 1. Schematic of the 1-D model used for analysis of the strain magnification. A trench is etched below the laser waveguide to concentrate stress where it is the most useful, and the device is bonded to a submount with a different thermal expansion coefficient.

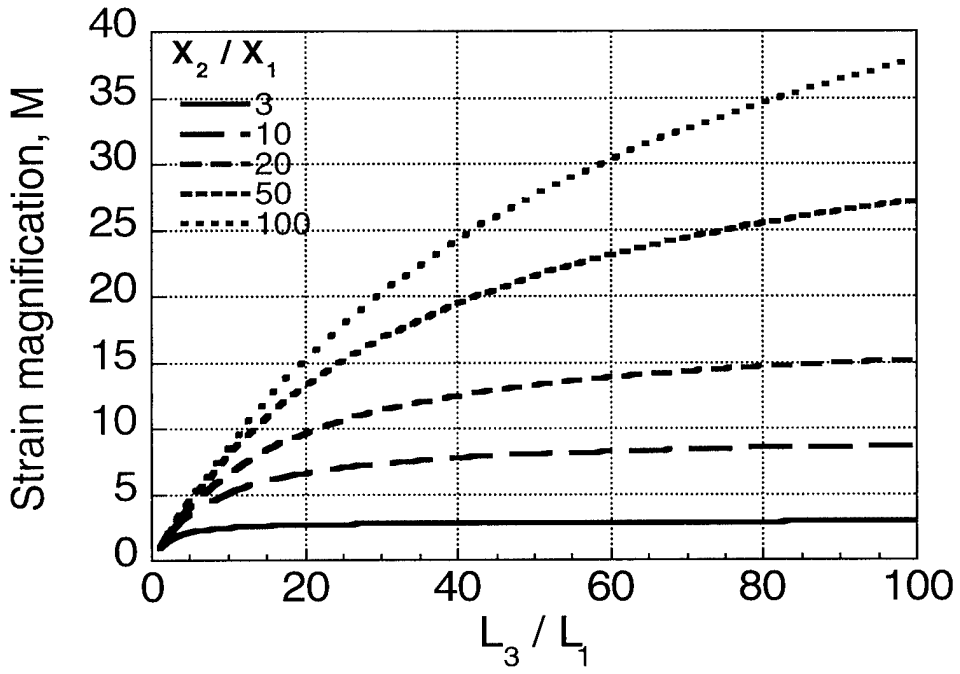

Fig. 2. Strain magnification as a function of the lengths of the etched and unetched portions. The parameter is the ratio of the thickness of the substrate and remaining web containing the laser waveguide.

The practical limit to X_2/X_1 is about 50, since the laser waveguide must be about 2 μm thick, and the substrate cannot be thicker than about 100 μm if it is to be cleaved. Thus, the magnification is limited to about 30. For ideal tuning reduction, assuming an InP substrate bonded to an Invar submount, the differential expansion is $3.7 \cdot 10^{-6}$/K, and the required magnification is 27, just within the limit predicted here. On the other hand, for tuning enhancement, assuming an InP substrate bonded to an aluminum submount, the differential expansion is $18 \cdot 10^{-6}$/K, and a doubling of the tuning rate requires a magnification of only 6.

Device Fabrication

We have obtained both tuning reduction and enhancement using the same strain-magnifying structure, but using different submounts. The lasers incorporated a Fabry Perot cavity oscillating in multiple longitudinal modes, rather than a DFB structure, for simplicity and to allow observation of any dispersion in the strain effects (none was observed.) The active region was a buried heterostructure with six GaInAs quantum wells, and 0.5% compressive biaxial strain incorporated during MOCVD growth. GaInAsP barriers with a bandgap wavelength λ_g=1.3 μm were used, with 170 nm thick waveguide layers of λ_g=1.25 μm, and InP cladding. A GaInAs stop-etch layer was grown 1.5 μm below the waveguide, for the subsequent trench etch. After laser regrowth and metallization, and after substrate thinning to 65 μm, a Si_3N_4 etch mask was patterned on the back side of the substrate, using IR alignment to position the mask opening directly beneath the waveguide. Pure HCl etched a crystallographic trench all the way to the stop-etch layer. We found it necessary to polish the substrate carefully, using colloidal silica and a bromine-methanol chemechanical polish, to avoid erratic etching due to subsurface damage. The mask width and substrate thickness determined the width of the trench at the stop etch layer, and our goal was to have the sloping sidewalls intersect the stop-etch layer leaving just a 5 μm width. However, the bromine-methanol polish was difficult to control, and we were not able to control the trench width accurately. Figure 3 shows the termination of a trench just below the stop etch layer. The stained active region is also visible, although this device would not lase due to a misaligned isolation implant, also visible in the photograph.

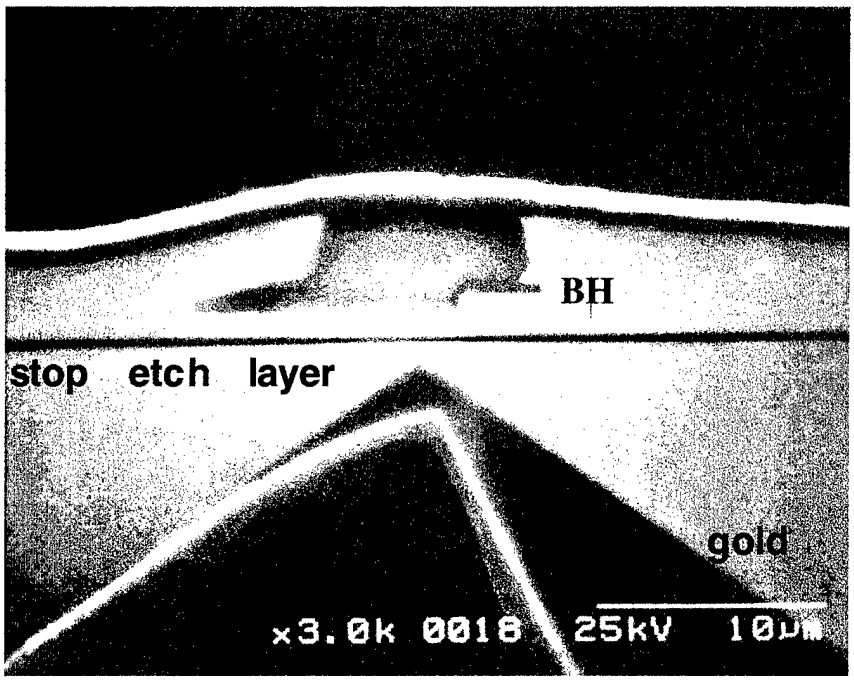

Figure 3. Strain-magnifying trench etched below a buried heterostructure (BH) active region. This device did not lase, due to a misaligned implantation made visible by a stain etch. The cleave was made across the trench, rather than across the reinforcing web, to study the trench bottom. A gold heat-spreading layer is seen tearing away from the trench sidewall.

The openings in the trench mask were interrupted every 900 µm along the length of the trench, for a distance of 200 µm, leaving an unetched rib spanning the trench. This rib strengthened the wafer against bending, so that it could be handled after etching. It also allows normal cleaving along the rib length for facet formation, although the lasers used in this work were first cleaved, then etched, using wax to protect the facets.

Tuning Enhancement

As discussed earlier, the differential expansion available with an aluminum submount should allow a significant increase in the temperature-tuning rate with only a modest strain magnification, so we explored this application first [2]. After fabrication of the lasers and trench etching, a cleaved bar was epoxied to an aluminum submount, as shown schematically in Fig. 4. Active lasers were distributed along the bar, separated by 150 µm. The width of the trench at the

stop-etch layer was 50 μm. The n-contact was obtained by burning out two adjacent lasers at the edge of the bar, and then using one shorted device for contact to the n-substrate. The response to temperature was measured on two oscillating modes, on either side of the 20°C gain peak, for the laser directly over the trench and for the lasers immediately to the side of the trench. The response was also measured on an identical bar, unetched, and bonded on only one side, to observe a "strain-free" device. The results are shown in Fig. 5. The unstrained device showed $d\lambda/dT$=0.10 nm/K, as is commonly observed. The device without strain magnification had $d\lambda dT$ =0.12 nm/K. The strain-magnified laser had $d\lambda dT$ =0.15 nm/K, 50% higher than a conventional laser.

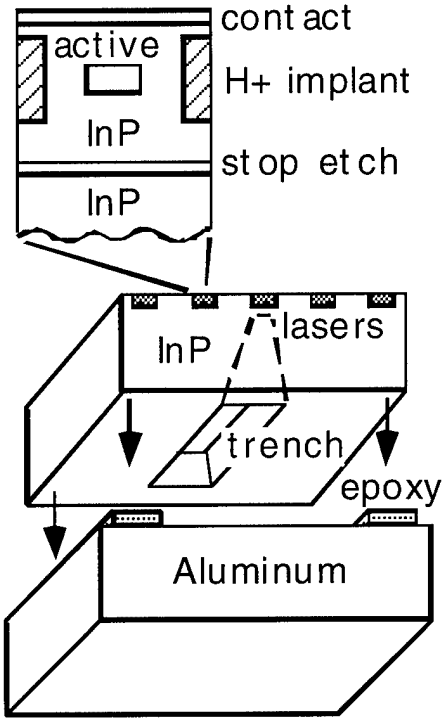

Fig. 4. Schematic of the strain-magnified laser bar bonded to a high-expansion submount.

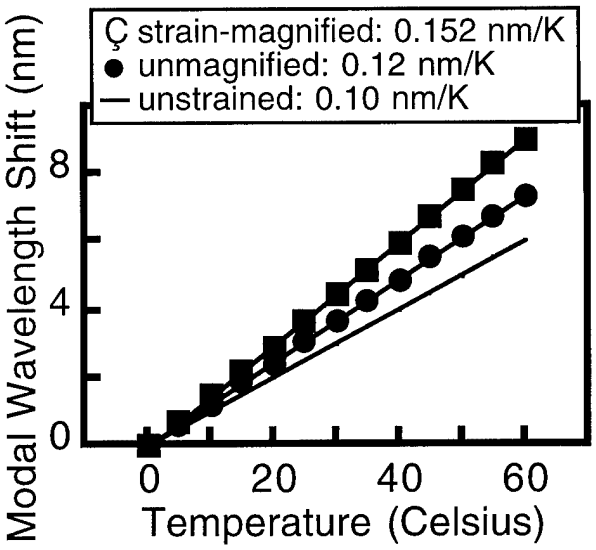

Fig. 5. Tuning enhancement with a strain-magnifying trench.

We measured $d\lambda/dT$ for all of the lasers along the bar, with the results shown in Fig. 6. As can be seen, only the single laser with the trench etch showed the magnification in $d\lambda/dT$.

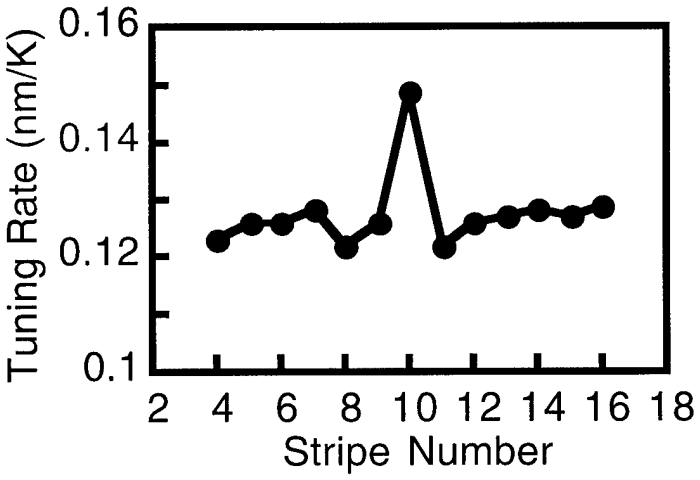

Fig. 6. Temperature response of all the stripes on the laser bar. The effect of the strain-magnifying trench below stripe 10 is clearly visible.

The measurements were performed under pulsed operation (500 ns at 10 kHz), to avoid any self-heating effects. We compared the increase in threshold current due to either increasing pulse width or increasing heatsink temperature, and found that the unetched laser's active region temperature increased 10 °C under CW operation (T_0=57 K), whereas the etched laser increased 13 °C (T_0=50 K). Thus, the InP cladding remaining after the trench etch is fairly effective at removing heat. This bar was mounted p-side up to allow access to all of the laser stripes. Naturally, a single die would be mounted p-down for improved heatsinking, and the temperature rise would be less.

We also fabricated strain-magnified ridge lasers without the stop-etch layer. The trench etch stopped directly on the quarternary waveguide layer, leaving only 2 μm of remaining material. This laser showed $d\lambda/dT$ =0.186 nm/K, nearly doubling the tuning rate. However, the severe index step at the semiconductor-air interface forced the optical field distribution away from the quantum wells, decreasing the modal gain and increasing the threshold current, so that the laser would not operate CW.

Since we have determined that a strain increase of $1.1 \cdot 10^{-4}$/K corresponds to a tuning rate of 0.1 nm/K [1], we conclude that the strain in the unetched lasers changed at $2.4 \cdot 10^{-5}$/K. This is a bit higher than the expected value based on the differential CTE between aluminum and InP, $1.8 \cdot 10^{-5}$/K. In a simple one dimensional approximation, the ratio of the strains in the etched and unetched lasers should be inversely proportional to their cross sections. If we include the reinforcing ribs, this is a factor of 17 in our experiments, so the magnified tensile strain due to differential expansion should be $3.1 \cdot 10^{-4}$/K. However, the observed strain based on tuning is only $5.5 \cdot 10^{-5}$/K. We suspect that the discrepancy is due to bending of the laser bar. The bar is contacted on its bottom surface, so the stretching force exerted by the submount applies a bending moment as well. We have analyzed this, based on handbook expressions for bending of beams [3, 4]. The U-channel formed by the waveguide and the reinforcing ribs has a neutral axis 26 μm below the waveguide, so that the strain in the waveguide due to bending alone is compressive at $-2.4 \cdot 10^{-4}$/K. The net tensile strain due to stretching and bending is then $7 \cdot 10^{-5}$/K. This would produce a net tuning rate of 0.164 nm/K, including the tuning due to temperature alone. This is in reasonable agreement with our measured value of 0.15 nm/K.

In practice, the laser would be bonded p-down, so that any bending would add to the tensile strain, rather than subtract from it. In this case, this simple model predicts a tuning rate of 0.60 nm/K, a six-fold increase over the usual value.

Tuning Reduction

We have also bonded a device identical to that described above, onto a submount made from the zero-expansion ceramic Zerodur, and relied on the small differential expansion between the InP and the Zerodur to produce an increasingly compressive strain with increasing temperature. Pulsed testing was performed again, with the results shown in Fig. 7. All of the stripes on the bar showed a tuning rate 10-15% lower than an unstressed laser, with an average $d\lambda/dT$ of 0.088 nm/K, compared to the usual 0.10 nm/K of an unstressed laser at this wavelength. The single stripe with the strain-magnifying trench tuned at 0.078 nm/K, a modest 22% reduction from the unstressed case. As with the tuning-enhanced laser, the effectiveness of the strain-magnifying trench is apparent, but not as great as predicted from the simple model. We again suspect that bending is negating much of the intended strain.

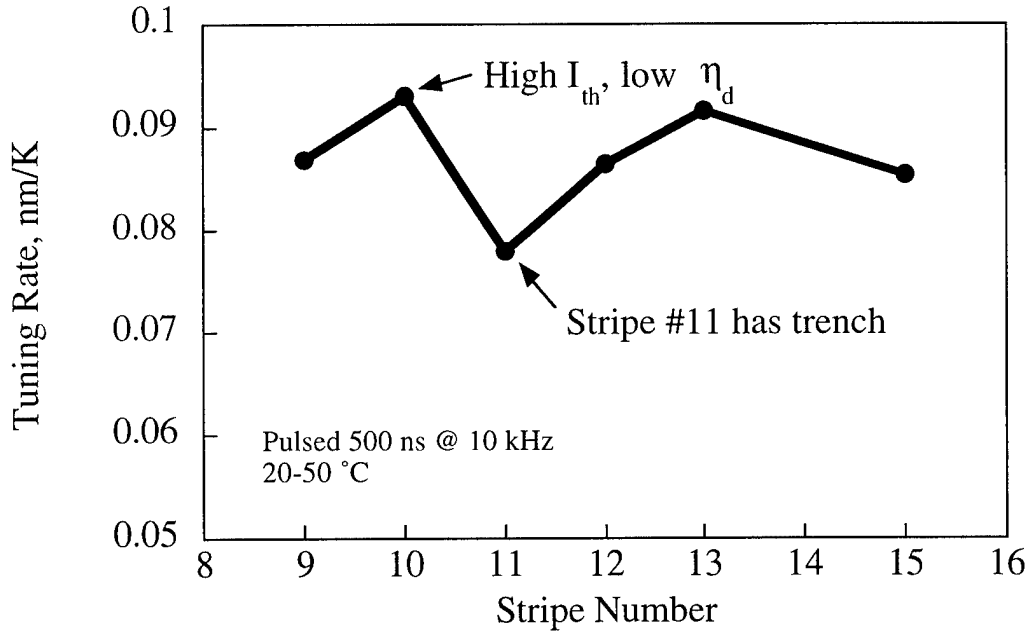

Fig. 7. Reduced tuning of a strain-magnified laser bonded to a zero-expansion submount. Stripe 10 had an anomalous threshold current and differential efficiency, and its tuning rate is excluded from the calculated average.

To eliminate this question of bending, we bonded a laser bar to a Zerodur submount as shown in Fig. 8, sandwiching the bar between a silicon brace at one end and an aluminum stress element at the other. The aluminum piece had a full 3 mm of unbonded length over which to expand. Thin layers of cyanoacrylate adhesive (superglue) buffered the ends of the fragile InP bar. The tuning response of this device is shown in Fig. 9. The initial tuning rate was only 0.004 nm/K, but rose sharply above 35 °C. When the device was then cooled down, the tuning rate was 0.0085 nm/K. The next heating cycle started with a tuning rate of 0.075 nm/K, the same as a laser on the bar without the strain-magnifying trench, and then decreased to 0.017 nm/K. This behavior clearly indicates some form of yielding, and indeed a crack was observed to grow roughly parallel to the laser stripe, near the outer edge of the trench.

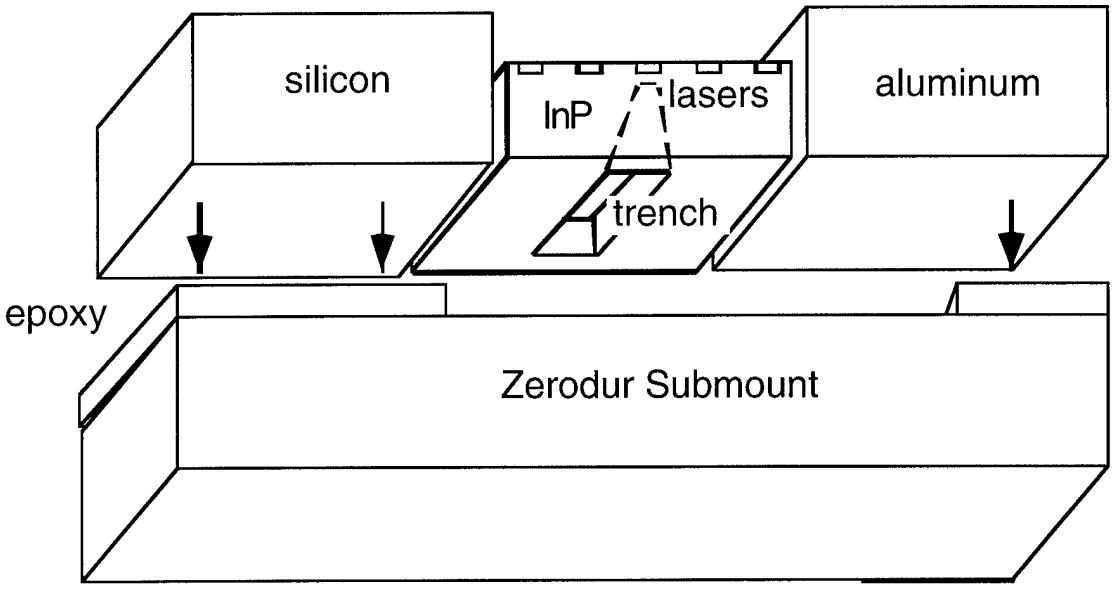

Fig. 8. Elimination of bending using side braces. The unsupported length of the aluminum stress element was 3 mm, and the laser bar length was approximately 4 mm.

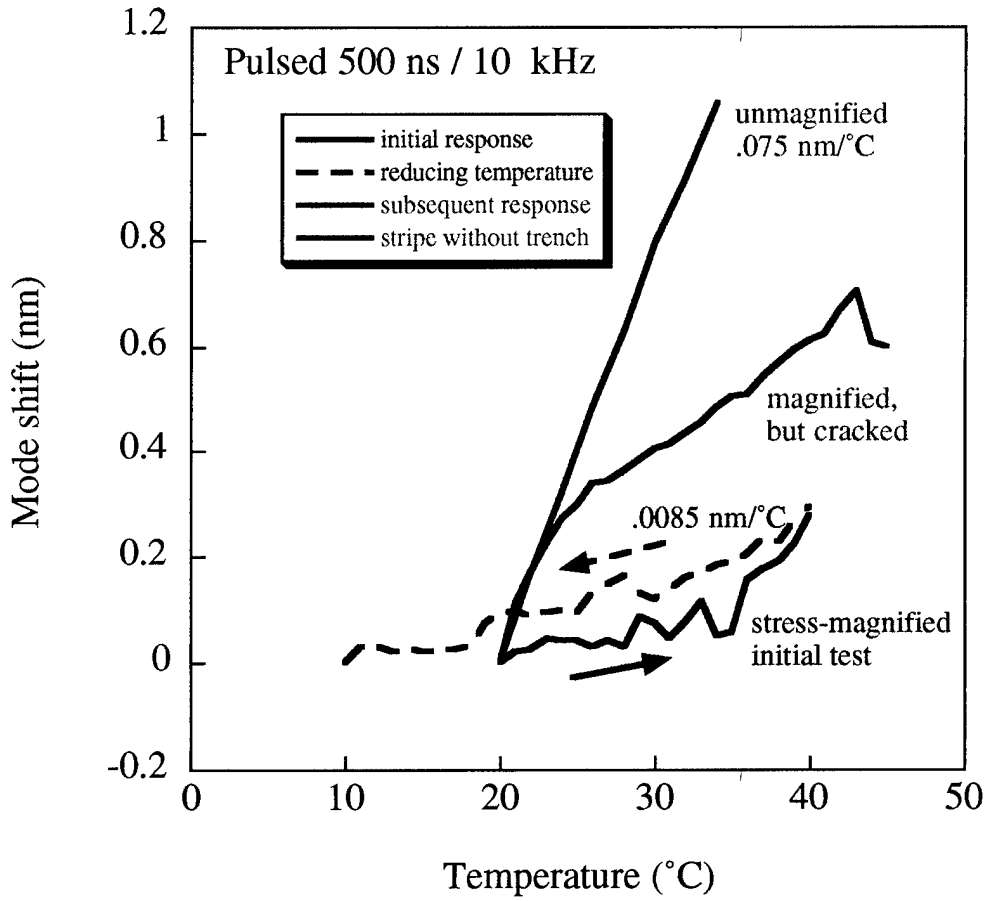

Fig. 9. Tuning response of a laser mounted on Zerodur, with side braces. Though the initial response was nearly ideally compensated, crack formation reduced the available strain.

Fracture

All of the devices that we tested failed by fracturing, with the crack beginning at the outer side of the trench. From the shift in modal wavelength before failure, we know that fracture occurred at strains well below 1%. This was true whether the device was in tension for tuning enhancement, or in compression for tuning reduction. It is not surprising that the devices loaded in tension failed, since the InP substrate is a brittle ceramic. Nor is it surprising that the crack initiated at the junction between the thick substrate and the thin trench bottom. But the failure of the devices loaded in compression was not as expected.

The bottom of the strain-magnifying trench, at the stop etch layer, was approximately 50 μm wide, but only 3 μm thick, and we should expect buckling of this membrane under compression. The critical strain for buckling, ε_{cr}, is given by [5]

$$\varepsilon_{cr} = \frac{\pi^2 h^2}{3L^2},$$

where h and L are the membrane thickness and length, respectively. In our case, this critical strain is 1.2%, well above the value obtained from the wavelength shift before failure. In addition, the buckling strain should be raised by the presence of the reinforcing webs along the facets.

We might also suspect that the bending of the structure might increase tensile strain on one side of the trench. Indeed, we calculated that in the enhanced-tuning device, the strain due to the bending moment was comparable to that due to direct tension, but was of the opposite sign on the top surface of the web, where the laser was. On the bottom surface, then, the bending leads to an additional tensile component, nearly doubling the strain. However, on the reduced-tuning device with direct compression applied by supporting braces, both surfaces should have been in compression at all times. We must conclude that local strain concentration due to irregular etching or defects contributes to the early fracture.

Monolithic Approaches

The submounts used in the preceding experiments were somewhat larger than typical submounts, but were small enough to be incorporated into some of the standard laser packages in use now. The bonding of the laser die to the submount is also not much different from normal bonding techniques, as long as no side bracing is required. Nonetheless, the die is large to accommodate the shear strain in the bond, and from the standpoint of manufacturing cost a monolithic approach is desirable. We explored some possible approaches.

The simplest step from hybrid assembly to a monolithic device would be to replace the high-expansion submount with a thick electroplated metal film. The necessary properties of this film would be a high expansion coefficient, and high stiffness to insure that the strain is in the laser and not in the stress-inducing film. While aluminum has a high expansion coefficient, it is

not particularly stiff, nor is it easily electroplated. Nickel is stiffer, and is easily plated, but has only half the expansion. Manganese has a coefficient of expansion equal to that of aluminum, and is very stiff as well. It has also been electroplated, although only for metal refining, not for electronic or mechanical purposes. We thus undertook an effort to electroplate manganese films and measure their mechanical properties.

We electroplated films from an aqueous solution of $MnSO_4$ (200 g/l) and $(NH_4)SO_4$ (150 g/l), onto glass substrates upon which a thin Cr/Au seed layer had been evaporated. Since the cell overvoltage exceeds the voltage needed to electrolyze water, plating was accompanied by sever bubbling. This bubbling was reduced, but not eliminated by adding H_2SeO_3 (0.5 g/l) to the solution. The resulting films were generally rough, and imbedded with nonmetallic deposits. Nontheless, we were able to deposit films up to several microns thick.

We measured the stress and thermal expansion of the plated films by measuring the curvature of the film and substrate as a function of temperature. The results are shown in Fig. 10, for different plating temperatures. The rate of change of stress with temperature should be[5]

$$\frac{d\sigma}{dT} = \frac{\Delta\alpha \cdot E_s}{1-\nu},$$

where σ is the stress, $\Delta\alpha$ is the differential expansion between the film and the substrate, E_s is the substrate Young's modulus, and ν is the substrate Poisson ratio. In this case, we calculate $d\sigma/dT$~3 MPa/K. The measured values, however are 10-15 MPa/K, and correspond to strain building at $d\varepsilon/dT$~5-7•10^{-5}/K, as shown in Fig. 11. This is 2-3 times larger than the differential expansion measured in bulk manganese. Similar results have been observed in evaporated SiO_2 films, but are not well understood. For our application, this anomaly is beneficial, as long as it is not accompanied by degradation of the film stiffness.

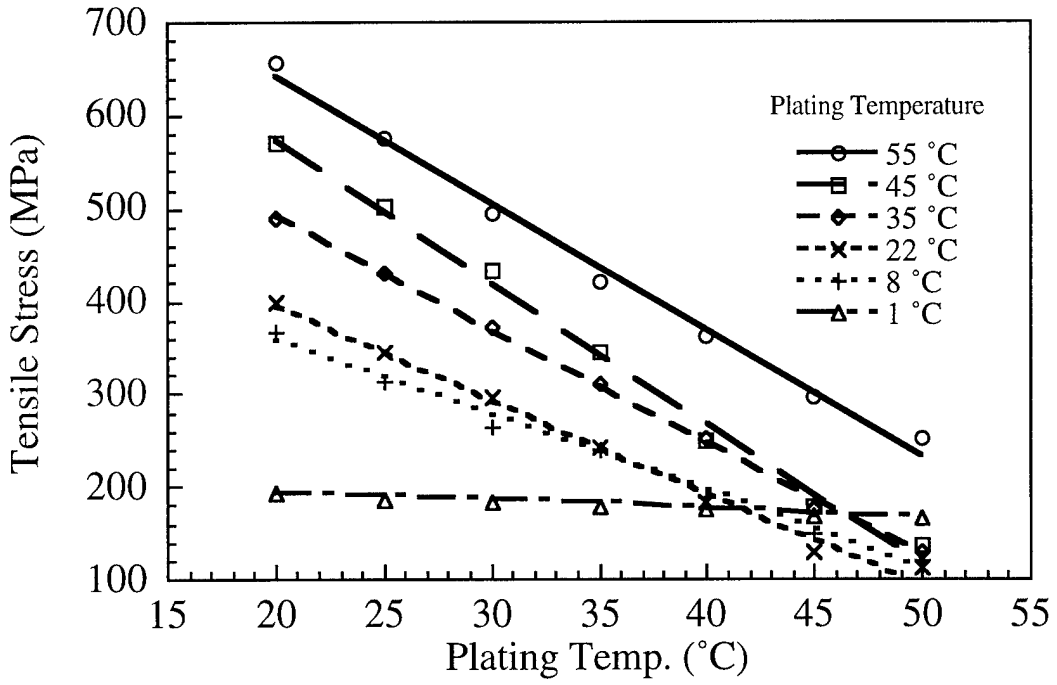

Fig. 10. Stress in electroplated manganese films.

We can no longer neglect the compliance of the stress-producing element when it is a film. From the expression for strain magnification, the film's compliance becomes significant when the ratio E_3X_3/E_1X_1 becomes small compared to the ideal magnification L_3/L_1. Thus, for a magnification of 6 (for tuning enhancement), and noting that E_3/E_1 is only 2, we should keep $X_3/X_1 >> 3$. Since X_1 is at least 2 μm, we would need a manganese film 6-10 μm thick to be at all effective, and tens of microns thick to neglect the film compliance. It appears that films this thick may be possible, although elevated plating temperatures will be required. Control of the residual stress at room temperature will be needed to avoid failure of the thick films, and this will require careful control of the purity and current density.

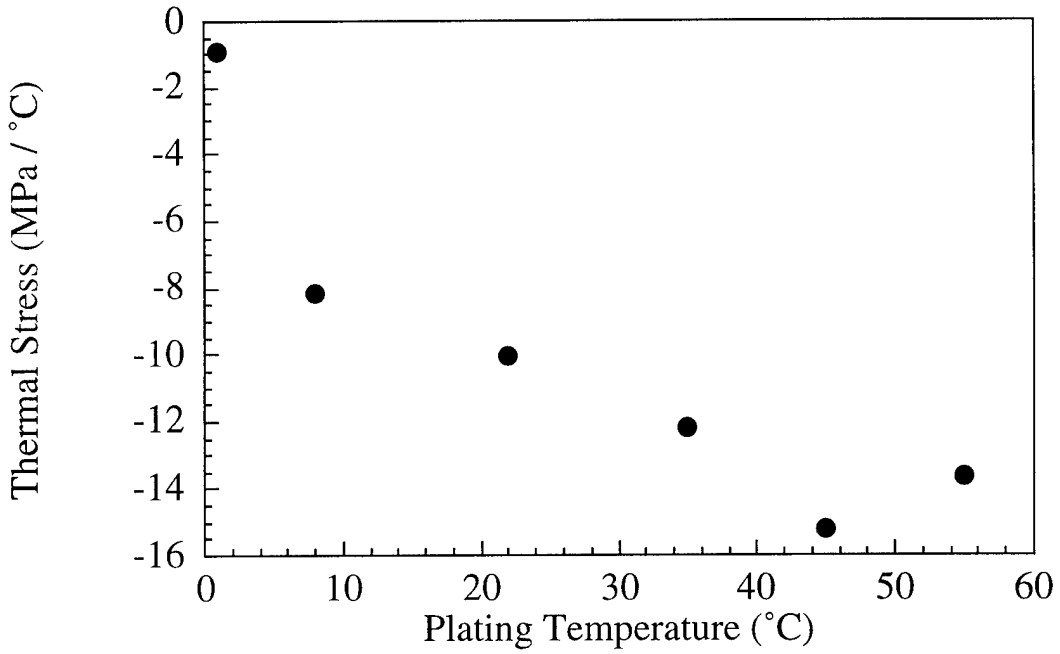

Fig. 11. Thermal stress in electroplated manganese films, as a function of plating temperature. The films are tensile, but become less tensile as the measurement temperature increases.

Conclusion

We have shown that temperature-dependent strain due to differential thermal expansion can be used to either increase or decrease the rate at which a diode laser's wavelength tunes with temperature. Both results would find use in optical communication systems, if they could be implemented in a reliable and cost-effective manner. Toward this end, we have developed a technique to magnify the effect of differential expansion by using a strain-concentrating trench in conjunction with a laser submount chosen for specific expansion properties. The trench is suitable for wafer-scale fabrication, and hybrid assembly to the submount is similar to standard packaging techniques.

We have shown that the considerable forces generated by differential expansion may be distributed over a wide bond area so that the shear loads on the bonds are small and the bond compliance does not limit the achievable strain. While this does require a large die size, this is seldom an issue in the final cost of fiber-coupled lasers.

To prove the efficacy of the strain-magnifying trench, we bonded our lasers with the epitaxial side up, to access both magnified and unmagnified lasers on the same bar. This did show the improvement due to the trench, but led to unintended bending of the bar which limited the net effect of the strain. The bending also contributed to premature failure due to fracture. We believe that epi-down bonding would improve both the performance and the reliability.

In fact, reliability remains the biggest obstacle to implementation of this technology. The brittle laser substrate cannot tolerate tensile strain, and so must be preloaded in compression to avoid tension under all operating *and storage* conditions. For enhanced-tuning devices in which the load becomes more tensile with increasing temperature, this compressive preload may be obtained by bonding at an elevated temperature. Just the opposite is needed for the reduced-tuning structure. It is also important to carefully control the width of the trench bottom so that the thin web that contains the laser waveguide does not buckle under the compressive load. This requires careful thinning and polishing of the substrate prior to the crystallographic trench etch, with a thickness accuracy of a few microns. Defects, or perhaps roughness, at the edges of the trench may also serve as localized stress concentrators and sites for crack initiation. These might be removed with a brief isotropic etch. But all of these improvements must be done before long-term reliability can even be tested. Thus, questions regarding fatigue and creep remain unanswered.

At this point the potential benefits of this technology must be weighed against advances in competing technologies; the reliability and cost of thermoelectric coolers continue to improve, so wavelength stabilization becomes easier using this old approach. And lasers with wide electrical tuning are becoming available, so that temperature tuning is no longer necessary. It may be that the strain-magnified laser is of more interest in sensor applications, increasing the sensitivity to external fields or forces.

References

[1]. D.A. Cohen and L.A. Coldren, "Passive Temperature Compensation of Uncooled GaInAsP-InP Diode Lasers using Thermal Stress," *IEEE Journal of Selected Topics in Quantum Electronics*, **3**, (2), April 1997, pp. 649-658.

[2]. D.A. Cohen, B. Mason, J. Dolan, C. Burns, L.A. Coldren, "Enhanced Wavelength Tuning of an InGaAsP-InP Laser with a Thermal-Strain-Magnifying Trench," *Applied Physics Letters*, **77**, (17), October 23, 2000.

[3]. A. Jensen and H. H. Chenoweth, Statics and Strength of Materials, 4th ed., McGraw-Hill, New York, 1983.

[4]. A. Blake, Handbook of Mechanics, Materials, and Structures, John Wiley and Sons, New York, 1985.

[5]. J.H. Faupel, Engineering Design, John Wiley and Sons, New York, 1964.